This is an open access article published under an ACS AuthorChoice License, which permits copying and redistribution of the article or any adaptations for non-commercial purposes.

ACS OMEGA

http://pubs.acs.org/journal/acsodf

Article

Cyclic Carbonate Formation from Epoxides and CO_2 Catalyzed by Sustainable Alkali Halide–Glycol Complexes: A DFT Study to Elucidate Reaction Mechanism and Catalytic Activity

Valeria Butera* and Hermann Detz

Cite This: *ACS Omega* 2020, 5, 18064–18072

Read Online

ACCESS | Metrics & More | Article Recommendations | Supporting Information

ABSTRACT: We provide a comprehensive DFT investigation of the mechanistic details of CO_2 fixation into styrene oxide to form styrene carbonate, catalyzed by potassium iodide–tetraethylene glycol complex. A detailed view on the intermediate steps of the overall reaction clarifies the role of hydroxyl substances as co-catalysts for the alkali halide-catalyzed cycloaddition. The increase of iodide nucleophilicity in presence of tetraethylene glycol is examined and rationalized by NBO and Hirshfeld charge analysis, and bond distances. We explore how different alkali metal salts and glycols affect the catalytic performance. Our results provide important hints on the synthesis of cyclic carbonates from CO_2 and epoxides promoted by alkali halides and glycol complexes, allowing the development of more efficient catalysts.

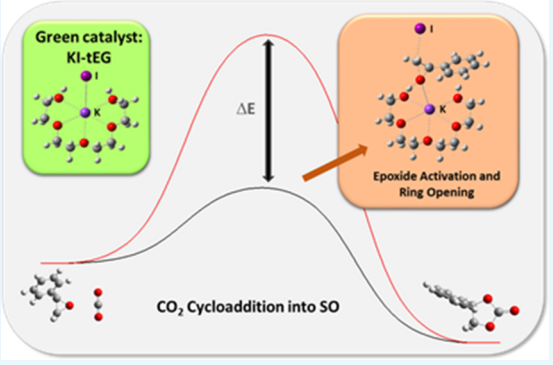

1. INTRODUCTION

The steady increase of carbon dioxide, CO_2, concentration released in the atmosphere is considered the main factor responsible for global climate changes. However, in spite of all the efforts to decrease its emissions, CO_2 can be considered as a low-cost, abundant, and renewable carbon source. In this context, great interest has been addressed to its potential use to produce materials of commercial interest.[1−6]

Its conversion into useful products and chemicals is unfortunately hindered by its high thermodynamic stability and therefore low reactivity. Hence, the field of green and sustainable chemistry is focusing much interest in developing efficient catalytic process for CO_2 conversion into valuable compounds.[7] Among these, increasing attention has been addressed to catalytic cycloaddition of CO_2 to epoxides, which leads to the production of cyclic carbonates and polycarbonates.[8−16] Cyclic carbonates are relevant chemical products with several applications and high utility in the industrial process.[17−21] Many different catalytic systems have been proposed, including ionic liquids,[22] bifunctional or binary complexes,[23,24] and quaternary onium salts, i.e., ammonium salts, which have shown high activity and stability for this reaction.[25] In a previous work,[26] we have investigated the fixation reaction of CO_2 into styrene oxide, SO, for the production of a styrene carbonate catalyzed by the nonsymmetrical aluminum catalyst Al1cat. The uncatalyzed reaction has been also investigated along with the binary system Al1cat/TBAB (TBAB = tetrabutylammonium bromide). In agreement with other previous theoretical investigations, our results have shown that the non-catalyzed reaction requires very high energy barriers that can be notably reduced thanks to the introduction of catalysts. Moreover, the results obtained by our quantum-mechanical investigation rationalized the experimental findings and provided an understanding of the reaction process at the molecular level. Our findings explained why the presence of the binary Al1cat/TBAB catalytic system facilitates the cycloaddition of CO_2 to styrene oxide in comparison with both uncatalyzed and TBAB- and Al1cat-catalyzed processes.

Among the several studied bifunctional quaternary onium catalysts, those containing iodide halide and having a hydroxy group have been found very efficient catalysts under mild reaction conditions for fixation of CO_2.[27] Alkali halides represent also potential nontoxic, cheap, abundant, and "green" catalysts for CO_2 cycloaddition reactions. Yet, their low activity requires the presence of hydroxyl substances, acting as co-catalyst, to improve the activity toward a CO_2 cycloaddition reaction.[28]

Lee et al.[29] reported the remarkable efficiency of bis-terminal hydroxy polyethers as a new class of an all-purpose promoter system. Their study was based on the two important concepts of "naked" and "flexible" halide ions. On one hand, alkali metal fluorides' solubility can be increased using crown ethers that

Received: April 7, 2020
Accepted: June 16, 2020
Published: July 13, 2020

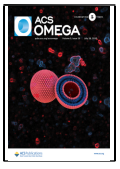

Downloaded via BRNO UNIV OF TECHNOLOGY on October 29, 2021 at 07:54:20 (UTC).
See https://pubs.acs.org/sharingguidelines for options on how to legitimately share published articles.

© 2020 American Chemical Society

https://dx.doi.org/10.1021/acsomega.0c01572
ACS Omega 2020, 5, 18064–18072

generate a "naked" fluoride ion. However, the strong basicity of fluoride limits their application in chemical reactions, leading to the formation of by-products. On the other hand, the use of bulky protic solvents and CsF leads to a reduced basicity of the nucleophile thanks to the formation of controlled hydrogen bonding, thus generating a "flexible" fluoride ion. Based on these observations, Lee et al.[29] designed bis-terminal hydroxy polyethers that act as multifunctional organic promoters in several organic reactions via a cooperative activation mechanism: the polyether chelates the cation acting as a Lewis base. Thanks to the notably reduced interaction between fluoride and potassium, the nucleophile is freed and the solubility of the salts is enhanced; simultaneously, a hydrogen bond is formed between fluoride anion and one of the two OH groups, thus reducing the nucleophile's basicity, while the second OH group most likely activates by hydrogen bonding the electrophile and, therefore, stabilize the transition state.

Based on these observations, recently, Kaneko and Shirakawa[30] have reported a practical method for the production of cyclic carbonates assisted by a potassium iodide tetraethylene glycol complex, KI-tEG, catalyst under mild reaction conditions (atmospheric pressure, 40 °C).

In their study, the authors confirm the production of a complex formed by tetraethylene glycol, tEG, and potassium salts[31−34] whose production contribute to increase iodide nucleophilic ability.[35,36] The authors also suggest that the activation of the epoxide substrates occur through hydrogen bond interactions with the terminal hydroxy groups of tEG. Kaneko and Shirakawa[30] also studied the effect of different glycols and alkali metal salts pointing out the importance of both the hydroxy groups of tetraethylene glycol, tEG, and the iodide of the alkali metal salt in the CO_2 fixation reaction. On the basis of their experimental findings, they proposed the reaction mechanism shown in Scheme 1.

Scheme 1. Proposed Catalytic Cycle

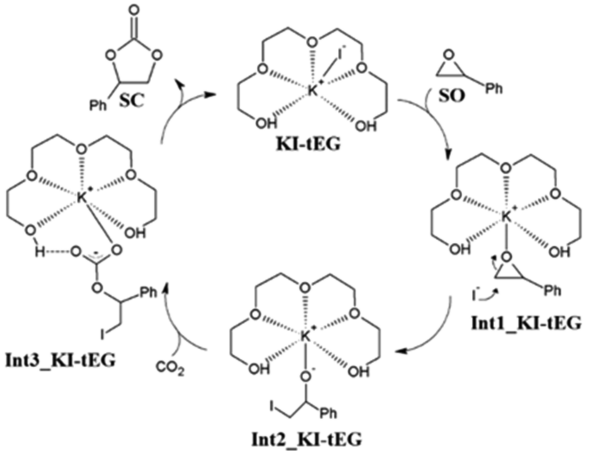

Even though it is well-known that compounds containing hydroxyl groups are very effective co-catalysts for the alkali halide-catalyzed cycloaddition, the involved reaction mechanism is unclear. Density functional theory (DFT) investigation furnishes a powerful approach to elucidate the details of the co-catalytic mechanism.

We present here a rigorous computational analysis of the suggested mechanistic scheme for the fixation process of CO_2 with SO chosen as model substrate for the formation of a cyclic carbonate via the use of a KI−tEG complex. Our choice was motivated by the sustainability of the KI-tEG catalyst used by Shirakawa's group.[30] In fact, polyethylene glycol (PEG) and, as mentioned above, alkali halides are non-toxic, bio-compatible, and bio-degradable and have become common alternative reaction media. Moreover, PEG is considered as a cheap, safe, low-cost, and abundantly available green solvent.[37]

Our quantum-mechanical investigation aims also to prove the improved efficiency of the catalytic activity of metal halides in presence of glycols and evaluate how tetraethylene glycol's presence can increase iodide nucleophilicity and reduce the involved energy barriers. Moreover, in the present computational investigation, we also explore how different alkali metal salts and glycols affect the catalytic performance.

The results obtained from our computational study contribute to a better understanding of cyclic carbonate production from CO_2 addition to epoxides. The knowledge gained from our quantum-mechanical investigation is indispensable for the improvement of the reaction conditions, and it can also be applied to a broader array of catalytic reactions.

2. RESULTS AND DISCUSSION

We provide a comprehensive DFT investigation of the reaction mechanism involved in the cyclic carbonate production by direct reaction of CO_2 and epoxide in the presence of MX-glycols (M = Na, K alkali metals; X = I, Cl, Br halides).

Styrene oxide was used as a model substrate. The overall reaction was first studied using the KI-tEG complex catalyst, and the rate determining step, RDS, was identified. To understand the effect of different glycols and alkali metal salts, the RDS was further investigated using different alkali metal salts and glycols. In order to evaluate the increase of the catalytic activity of the KI-tEG complex rather than KI metal salt alone, the reaction was also studied in the absence of glycol.

The uncatalyzed mechanism has been already investigated using several computational protocols. Applying the B3LYP/6-31G** computational protocol, the computed gas-phase, zero-point-corrected barriers for the α and β pathways are determined to be 45.7 and 60.8 kcal/mol, respectively.[26] Zhang and co-workers[22d)] report energy barrier values of 53.4 and 58.1 kcal/mol for the α and β pathways, respectively, calculated using the B3PW91 functional and 6-311++G (d, p) basis set. These results confirm that the uncatalyzed process involves very high energy barriers, and, therefore, catalysts need to be employed to reduce the involved energy.

In the next paragraph, we will first discuss the reaction between SO and KI. The following paragraph will present the details of the reaction mechanism, leading to the final cyclic carbonate product from styrene oxide and KI-tEG. The third and fourth paragraphs will clarify how the reaction mechanism and related RDS is influenced by the use of different alkali metal salts and glycols, respectively.

2.1. KI-Catalyzed Reaction. Previous experimental reports observed that almost no reaction occurs when a mixture of styrene oxide and KI alone was stirred for 24 h at room temperature (25 °C) under a CO_2 atmosphere (1 atm, using a balloon), mainly because of the low reactivity and solubility of KI under the reaction conditions.[30]

Figure 1 shows the free-energy profiles along with the intercepted minima and transition states. The sum of the isolated reactant energies, KI, CO_2, and SO, is set as zero for the calculation of relative free energies. Our DFT calculations

https://dx.doi.org/10.1021/acsomega.0c01572
ACS Omega 2020, 5, 18064−18072

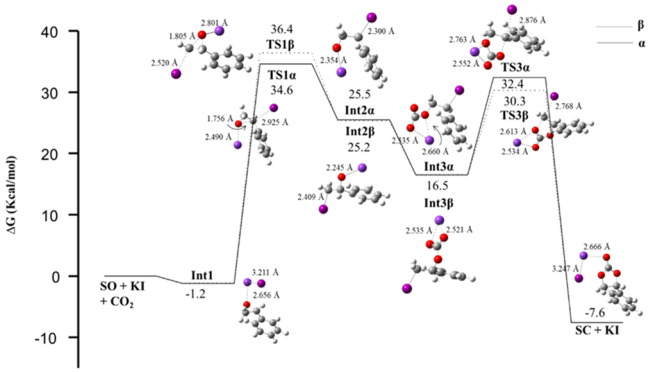

Figure 1. Free-energy surface alongside optimized structures of minima and transition states for the KI-catalyzed fixation of CO_2 with SO. The attacks on both Cα (solid line) and Cβ (dashed line) carbon of epoxide are reported. Energies are given in kcal/mol and relative to the reactants' asymptote.

show that when SO is added to KI, an intermediate, SO−KI, is formed. Such an intermediate, which lies at 1.2 kcal/mol below the entrance channel of the reaction, shows an O−K interaction between the O atom of styrene oxide and potassium, whose bond distance is 2.656 Å. The subsequent step is the ring opening occurring by nucleophilic attack of the iodide on the epoxide. Because of the presence of two different C atoms on the styrene oxide, two possible pathways need to be considered: the α pathway corresponds to I^- nucleophilic attack on the α carbon (most substituted carbon) of the styrene epoxide. The β considers the same nucleophilic attack on the β carbon (least substituted carbon). An energy barrier of 35.8 kcal/mol has been calculated for the α route that is about 2.0 kcal/mol more favored than the β pathway.

To confirm our results, we have also computed the energy barriers considering the commonly used B3LYP[38a),b)] functional and ω-B97XD[38c)] functional, which uses a version of Grimme's D2 dispersion mode. Following these computational protocols, the α pathway was identified as the favored one with computed energy barriers of 34.2 and 37.7 kcal/mol with B3LYP and ω-B97XD functionals, respectively. The alternative β route requires overcoming energy barriers of 36.3 kcal/mol when the B3LYP functional is used and 43.6 kcal/mol with ω-B97XD functional. These results are summarized in Table S1 in the Supporting Information. This difference was explained by NBO charge analysis[39] that shows a more negative charge on Cβ favoring the iodide nucleophilic attack on the more positive Cα (see Figure S1 reported in the Supporting Information, SI).

Han and collaborators[28] have studied the cycloaddition of CO_2 with propylene oxide, PO, catalyzed by KI. Three different reaction mechanisms have been proposed, and an energy barrier of 37.6 kcal/mol has been calculated for the pathway analogous to our β pathway. The overcoming of these barriers leads to the formation of an oxi-anion species labeled Int2α and Int2β, which are very endothermic with respect to the previous intermediates and lies at 25.5 and 25.3 kcal/mol, respectively.

Even though the ring opening steps have shown very high energy barriers, we decided to investigate also the subsequent steps leading to the final cyclic carbonate product. Our calculations show that the insertion of a CO_2 molecule onto the oxi-anion occurs without the existence of any transition state and leads to the formation of more stable linear carbonate intermediates, Int3α and Int3β, whose energy are 16.5 kcal/mol above the reactants' asymptote. Similar results were obtained by Han and co-workers[28] who attributed the lack of a TS to the large negative charge gained by the oxygen atom of the formed oxi-anion species, suggesting that the epoxy ring opening step is more important compared to the step of electrophilic attack of CO_2.

The next and final step leads to the formation, of the cyclic carbonate product along both α and β pathways, via the transition states TS3α and TS3β, corresponding to the concerted ring closure and release of the iodide anion. The corresponding computed barriers are 15.9 and 13.8 kcal/mol, respectively.

All these results confirm that KI salt alone has the ability to reduce the energy barrier of the cycloaddition of CO_2 with epoxides of about 20 kcal/mol thanks to the synergistic action of the potassium cation and iodide. Specifically, in the ring opening step, while the I anion attacks the epoxide carbon leading to the epoxy ring opening, potassium cation establishes an electrostatic attraction stabilizing the anionic group. In the subsequent cyclic carbonate formation step, the presence of K cation facilitates the release of the iodide, which is itself also a good leaving group, by electrostatic attraction. However, the involved energy barriers are still too high and co-catalysts have to be introduced to reduce the cycloaddition reaction energy barriers. As we will discuss in detail in the next paragraph, the nucleophilicity of halides in alkali metal salts is notably increased when bis-terminal hydroxy polyethers are added to the reaction system, leading to the formation of the MX-glycol complex, where M is an alkali metal and X a halide.[27,28,30]

On the basis of those suggestions, we address catalytic performance changes when the reaction is performed using KI alkali metal salt in the presence of tetra-ethylene glycol.

2.2. KI-tEG Reaction. In the proposed catalytic cycle, shown in Scheme 1, the authors[30] suggested that the epoxide is activated via double hydrogen bonding with hydroxy groups of tetraethylene glycol (Int1_KI-tEG). The activated epoxide then undergoes nucleophilic attack from an iodide anion to form Int2_KI-tEG. The reactive alkoxide in Int2_KI-tEG attacks CO_2 to yield Int3_KI-tEG. The intramolecular ring-closing of the last intermediate forms the final cyclic carbonate product along with the regeneration of the KI−tetraethylene glycol complex catalyst.

Figures 2 and 3 outlines the free-energy profile and the optimized structures of the intercepted intermediates and

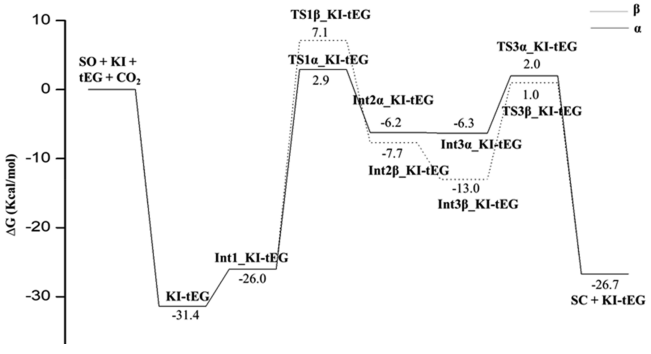

Figure 2. Free-energy surface for the KI-catalyzed fixation of CO_2 with SO. The attacks on both Cα (solid line) and Cβ (dashed line) carbon of epoxide are reported. Energies are given in kcal/mol and relative to the reactants' asymptote.

https://dx.doi.org/10.1021/acsomega.0c01572
ACS Omega 2020, 5, 18064−18072

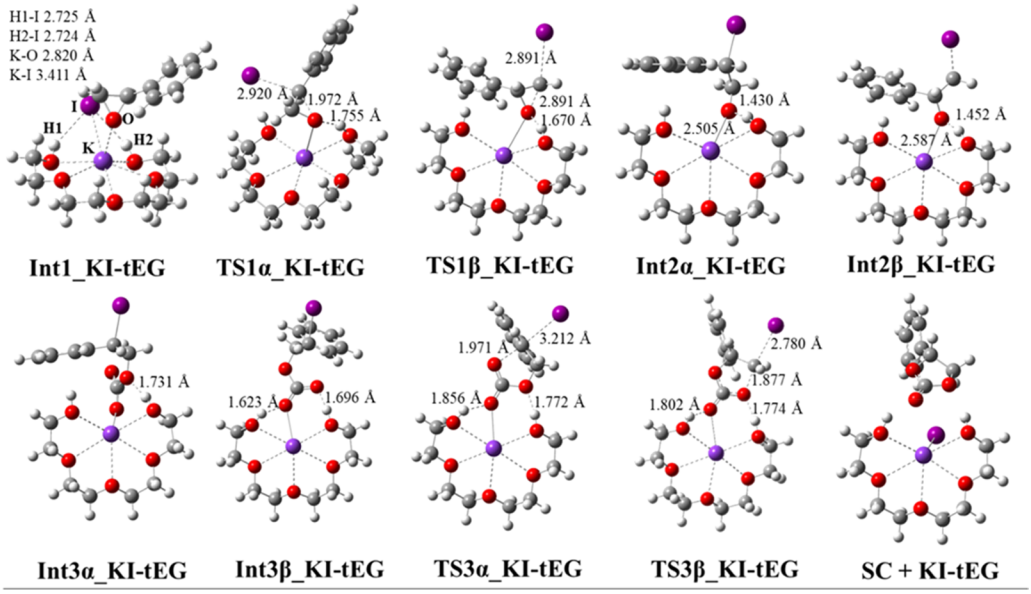

Figure 3. Optimized structures of minima and transition states for KI-tEG-catalyzed fixation of CO_2 with SO along both α and β pathways.

transitions states, respectively. The sum of the isolated reactants energies, Glycol, KI, CO_2, and SO, is set as zero for the calculation of relative free energies. We first investigated the formation of the KI-tEG complex catalyst. In agreement with the experimental suggestions, our calculations show that K cation interacts with the oxygen atoms of the glycol, while the H atoms of the hydroxy groups of tEG interact with the iodide. Those interactions contribute to significantly stabilize the formed intermediate whose energy lies 31.4 kcal/mol below the reference energy of the separated reactants.

In order to confirm the suggested lower nucleophilicity of iodide anion in KI alone with respect to the KI-tEG complex, NBO charge analysis[39] was performed. As reported in Table 1,

Table 1. Potassium and Iodine Calculated NBO and Hirshfeld Charges and K−I Bond Lengths of the KI Salt and KI-tEG Complex

	NBO Charges		Hirshfeld Charges		K-I Bond Distance (Å)
	K	I	K	I	
	0.939	-0.939	0.660	-0.660	3.360
	0.902	-0.865	0.381	-0.534	3.469

our DFT calculations show that the negative charge on iodide and the positive charge on potassium in the KI-tEG complex (−0.865 and +0.902) are both lower than that in KI (−0.939 and 0.939). Same trends are obtained when Hirshfeld charge analysis[40] is performed. However, the optimized cluster structures of the KI and KI-tEG complex show that the K−I bond distance is 0.109 Å longer in the KI-tEG complex than in KI. Therefore, tetraethylene glycol molecule acts as a Lewis base toward potassium cation dramatically lowering the electrostatic interaction with I anion and thereby "freeing" the nucleophile I^-. Similar conclusions were obtained by Han et al.[28] in their study of the cycloaddition of CO_2 and PO with KI as the catalyst.

The addition of the epoxide to the reaction system leads to the first intermediate, Int1_KI-tEG. Such an intermediate is 5.4 kcal/mol less stable than the KI-tEG mainly because of the entropic cost for bringing together KI-tEG and SO.

The optimized structure of Int1_KI-tEG shows that the activation of the epoxide occurs through the interaction of the O atom with the potassium cation, whose O−K bond distance is 2.820 Å, while both the hydroxyl groups are still involved in the interactions with iodine. This result is different from what is suggested by Kaneko and Shirakawa.[30] As mentioned above, the authors' suggestion is that styrene epoxide is activated via double hydrogen bonding with hydroxy groups of tEG. In another DFT investigation of the reaction of C_3H_7OMs with KF in tetraethylene glycol, Lee and co-workers[29] observed that only of the two OH groups of tetraethylene glycol forms a hydrogen bond with the fluoride nucleophile while the second OH group simultaneously activates the electrophile by hydrogen bonding toward the nucleophilic attacks of the fluoride.

Once Int1_KI-tEG is formed, the reaction proceeds through the epoxide ring opening by nucleophilic attack of the iodide ion. As already discussed in the previous paragraph, two pathways, α and β, have to be taken into account: I^- nucleophilic attack on the most substituted α carbon of the styrene epoxide (α pathway) and nucleophilic attack on the less substituted β carbon (β pathway). The calculated free-energy barriers are 28.9 kcal/mol for the α pathway and 33.1 kcal/mol for the β pathway, therefore favoring the α route by ∼4 kcal/mol. NBO charge analysis[39] shows a more negative charge on Cβ favoring the iodide nucleophilic attack on the more positive Cα (see Figure S2 reported in the Supporting Information, SI) as already found for the KI-catalyzed system discussed previously. In the involved transition states, the unique imaginary vibrational frequency corresponds to the contemporary breaking of the C−O bond of the epoxide and the simultaneous formation of I-Cα (351.96i cm^{-1}) in TS1α_KI-tEG and I-Cβ (422.85i cm^{-1}) in TS1β_KI-tEG. Both the optimized structures of TS1α_KI-tEG and TS1β_KI-

https://dx.doi.org/10.1021/acsomega.0c01572
ACS Omega 2020, 5, 18064−18072

tEG show that the negative charge transferred to the O atom of the forming oxi-anion is stabilized by a hydrogen bond that involves one of the two glycol's hydroxyl groups. Therefore, the experimental suggestion of epoxide activation through H bond interactions can be confirmed by our DFT results as a way to stabilize the involved TS. This corroborates the conclusions by Lee et al.[29]

These hydrogen bonding interactions are also found in all the subsequent intercepted TSs and intermediates along the overall reaction. The first step of the studied mechanisms represents the rate determining step for both α and β routes. In the formed intermediates, Int2α-KI-tEG and Int2β-KI-tEG, which lie at −6.2 and − 7.7 kcal/mol, respectively, the oxi-anion species coordinates to the potassium cation. As already seen for the KI-catalyzed reaction, the insertion of the CO_2 molecule onto the oxi-anion occurs without the existence of any transition state and the linear carbonate intermediates, Int3α-KI-tEG and Int3β-KI-tEG, are formed. The computed energy stabilization of Int3β-KI-tEG is 6.7 kcal/mol higher than that of Int3α-KI-tEG thanks to the contribution of a further O···HO interaction that is not present in the α intermediate (see Figure 2). The second and last step of the reaction mechanism corresponds to the ring closure and simultaneous release of iodide anion occurring through transition states TS3α-KI-tEG and TS3β-KI-tEG. The imaginary frequencies at 303.8i cm^{-1} for the α pathway and 412.8i cm^{-1} for the β route are associated to the formation of new C−O and contemporaneous C−I bond's breaking. The energy barriers computed for this step are 8.3 and 14.0 kcal/mol along the α and β paths, respectively. These results show that also the ring closing step is favored along the α pathway.

Therefore, our DFT results confirm the experimental findings showing that addition of tEG to KI results in improving significantly the catalytic performance. In fact, the energy barrier for the RDS in the presence of the KI-tEG complex is 6.9 kcal/mol lower than with KI alone.

2.3. Effect of Other Alkali Metal Salts. In order to evaluate the effect of different alkali metal salts, the reaction was investigated in the presence of KCl, KBr, and NaI salts. Experimentally, low reactivities (∼0 and 4% yield) were observed with KCl- and KBr-tEG complexes. On the other hand, the sodium iodide (NaI) complex gave comparable results (68% yield) as in the case of the KI-tEG complex.[30]

These trends were explained by the better ability of iodide as the leaving group and by the lower coordination ability of hydroxy groups.[41]

In our DFT investigation, we first focused on the rate determining step that, as mentioned above, corresponds to the ring opening by nucleophilic attack of the halide. However, only the most favored α pathway has been investigated. Table 2 reports the calculated formation energies of MX-glycol complex (G_{form}) calculated as the difference between the energies of MX-glycol complexes and the sum of the separated energies of MX and glycols:

$$G_{form} = G(\text{MX} - \text{glycol complex}) - [G(\text{MX}) + G(\text{glycol})] \quad (1)$$

The computed barriers for the rate determining step (ΔG RDS) for all the alkali metal salts and for the carbonate cycle formations corresponding to the final step of the reaction mechanism (ΔG FS) are also reported.

The free-energy barrier for the reaction catalyzed in the presence of NaI is very similar to that of KI (28.5 and 29.0 kcal/mol). On the other hand, the energy barriers are much higher when the reaction is performed in the presence of KBr and KCl whose values are 44.2 and 40.8 kcal/mol, respectively. Our results confirm the observed experimental findings showing a lower reactivity of KBr and KCl catalysts in comparison with KI and NaI.

As mentioned above, the better performance of the iodide anion was explained in terms of lower coordination ability of hydroxy groups in the first formed intermediate, Int1, and better ability of I^- as the leaving group.

We, therefore, investigated these two aspects computationally. First, we compared the optimized structures of Int1 that are shown in Figure 4. In Int1-KI-tEG, both Iodide and SO are

Table 2. Calculated Formation Energies (G_{form}) of the MX-Glycol Complex and Energy Barriers of the Rate Determining Step (ΔG RDS) and Final Step (ΔG FS) Related to KCl, KBr, NaI, and KI Catalysts

parameter	KI	NaI	KBr	KCI
G_{form} (kcal/mol)	−31.4	38.1	−41.8	−39.5
$\triangle G$ RDS (kcal/mol)	29.0	28.5	44.2	40.8
$\triangle G$ FS (kcal/mol)	8.3	14.1	27.0	28.4

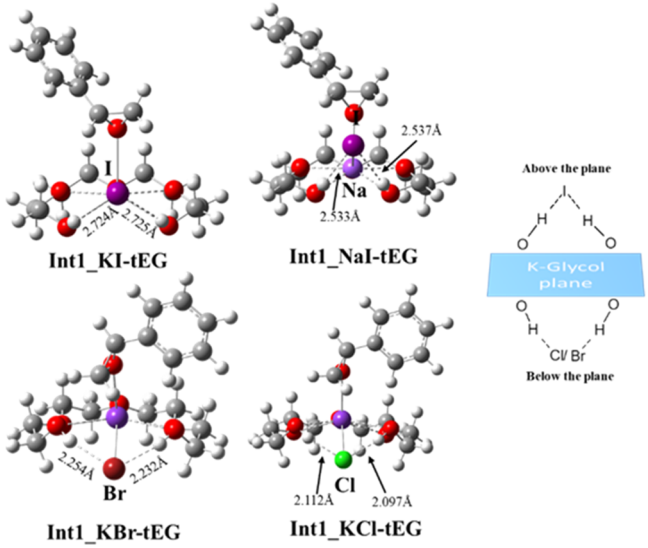

Figure 4. Optimized structures of Int1-KI-tEG, Int1-NaI-tEG, Int1-KCl-tEG, and Int1-KBr-tEG along with OH···X bond distances.

above the plane formed by K-glycol, and the hydrogen atoms of the OH groups are directed toward the iodide anion establishing H bonds whose values are 2.722 Å (2.725 Å.) Int1-NaI-tEG shows an identical structure with OH···I bonds that are ∼0.18 Å shorter. On the other hand, Int1-KCl-tEG and Int1-KBr-tEG show different structures in which the halide anion lies below the K-glycol plane. The hydroxyl groups, pointing toward the anions, establish stronger H bonds as underlined by the shorter OH···Cl and OH···Br bond distances of 0.2097 (2.112) and 0.232 Å (2.254 Å), respectively. The longest X···HO hydrogen bond interactions in I-based intermediates explains the suggested lower hydroxyl coordination ability.

We then calculated the energy barriers (ΔG FS reported in Table 2) involved in the release of the halide leaving groups

https://dx.doi.org/10.1021/acsomega.0c01572
ACS Omega 2020, 5, 18064−18072

that correspond to the final step of the already discussed reaction mechanism. In agreement with the experimental suggestions, our DFT results show that iodide is the best leaving group as confirmed by the lower energy barriers computed for KI-tEG and NaI-tEG complexes that are 8.3 and 14.1 kcal/mol, respectively. However, when the reaction is performed in the presence of KBr-tEG, the involved energy barrier becomes 27.0 Kcal/mol. Chloride is the worst leaving group with an energy barrier that is 1.4 kcal/mol higher than bromide.

2.4. Effect of Glycols. In order to understand the glycol effect, we have also studied the reaction using ethylene glycol, EG, and 18-crown-6 complex,18-c-6. The latter one has no OH groups, and it has been chosen to clarify the role of the hydroxyl groups in the catalysis. In both cases, KI salt was used and only the RDS was studied.

A low yield of only 6% was observed experimentally in the presence of ethylene glycol. This yield slightly increases to 17 and 24% when dimethyl ether glycol and 18-crown-6 complexes are used, respectively. Those experimental findings could confirm the important role of the H atoms in the catalytic activity.[30]

Our computed results show that the formation of the KI-18-c-6 complex, the energy of which is at 25.6 kcal/mol below the entrance channel of the reaction, is a highly exothermic process. On the other hand, KI-EG production involves a stabilization energy of 12.4 kcal/mol relative to the reactants' asymptote. This high difference in terms of stabilization energy of the formed complexes is explained by the presence of six oxygen atoms in 18-c-6 molecule that interact with the potassium cation located in the center of the 18-c-6 ring. The smaller EG molecule contains only two O atoms that interact with K.

The subsequent Int1-KI-18-c-6, is 6.2 kcal/mol is less stable than the previous one because of the entropic cost to bring SO close to KI-18-c-6. However, this entropic contribution is not significant in the case of Int1-KI-EG production. The involved energy barriers for the formation of Int2-KI-18-c-6 and Int2-KI- EG are 31.5 and 37.1 kcal/mol, respectively. Both the formed intermediates Int2-KI-18-c-6 and Int2-KI- EG are above the reactants' asymptote, lying at 8.5 and 19.4 kcal/mol, respectively. Also in this case, the bigger 18-c-6 molecule can stabilize the intermediate through O−K interactions better than the small ethylene glycol. All the discussed results are summarized in Figure 5 that shows the free energy profile and the intermediates and TSs involved in the rate determining step.

The outcomes of the computational analysis carried out so far are in agreement with the experimental findings confirming that 18-c-6 complex is a better glycol for this reaction than EG.

Moreover, the stabilization energy of the KI-18-c-6 complex is ∼6 kcal/mol lower than KI-tEG, while its calculated barrier for the RDS is 2.5 kcal/mol higher than KI-tEG. This different behavior can be attributed to the lack of OH groups in the 18-crown-6 complex that, as suggested by experiments, are important for the efficient promotion of the reaction.

3. CONCLUSIONS

We provide a rigorous quantum-mechanical investigation of the mechanism of the cycloaddition of CO_2 to styrene oxide, catalyzed by the bifunctional KI-tEG catalyst system. The outcomes of the computational analysis conducted here confirm the experimental trends showing that KI alone is not

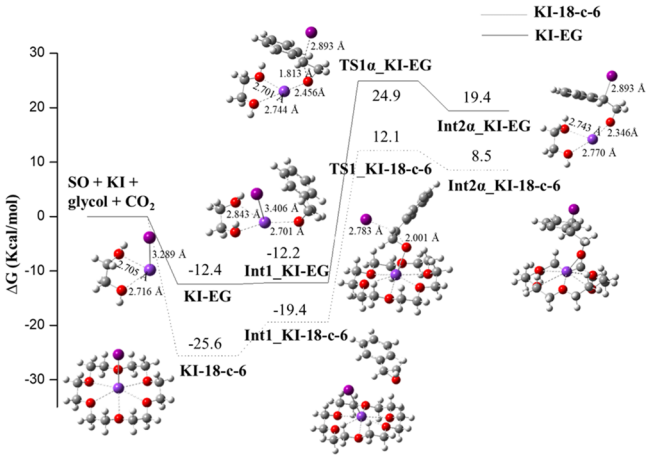

Figure 5. Free-energy surface alongside optimized structures of minima and the transition state for KI-EG (solid line)- and KI-18-c-6 (dashed line)-catalyzed ring opening step on Cα carbon of SO. Energies are given in kcal/mol and relative to the reactants' asymptote.

a good catalyst for this reaction. However, when tEG is added and KI-tEG complex is formed, the energy barrier for the epoxide opening with consequent formation of an oxi-anion species is ∼7 kcal/mol lower. Our DFT calculations confirm the experimental findings showing that tetraethylene glycol forms a complex with potassium iodide that significantly increases the nucleophilic ability of the iodide anion. In fact, the tetraethylene glycol molecule acts as a Lewis base toward potassium cation dramatically lowering its electrostatic interaction with I anion and thereby "freeing" the nucleophile, I^-. These conclusions were confirmed by the decreased negative charge on I^- and positive charge on K^+ calculated by NBO and Hirshfeld charge analysis and longer K−I bond distances in KI-tEG complex with respect to KI alone that corresponds to a weaker interaction between the two ions in KI-tEG than in KI.

The better catalytic performance of KI and NaI in comparison with KBr and KCl observed experimentally in terms of higher yields of iodide alkali salts was confirmed by our computational analysis showing the involvement of higher energy barriers when bromide and chloride salts are used.

The high computed energy barrier of 37.1 kcal/mol confirms the reported experimental yield of 6% when the reaction is performed using simple ethylene glycol and KI. Moreover, our DFT calculations reveal that the energy stabilization of KI-EG complex is the lowest among all the studied systems. The reason behind that is related to the small size of ethylene glycol with respect to the other investigated glycols and, therefore, its incapacity to establish interactions that stabilize the formed complex and all the following stationary points intercepted along the reaction path. On the other hand, 18-c-6 glycol misses OH groups involved in the formation of strong H bonds that contribute to the activation of the epoxide substrate and stabilization of all the involved stationary points. However, thanks to the presence of six O atoms in its ring, 18-c-6 glycol interacts with the potassium cation located in the center of the 18-c-6 ring, stabilizing the formed complex much more than ethylene glycol. Moreover, the additional oxygen atom of 18-c-6 glycol and the consequent formation of a further O−K interaction, plus the capability of 18-c-6 to "encapsulate" a potassium cation, compensates the lack of H bonds leading to

https://dx.doi.org/10.1021/acsomega.0c01572
ACS Omega 2020, 5, 18064−18072

a calculated energy barrier for the RDS that is only 2.5 kcal/mol higher than KI-tEG,

The computational results presented here offer an important rationalization of previous experimental observations and allow the development of more efficient catalysts for the synthesis of styrene carbonate via the reaction of styrene oxide and CO_2 in the presence of KI-glycol complex catalysts. These findings are furthermore relevant for a more complete understanding of the cyclic carbonates formation reaction using CO_2 as reactant.

4. COMPUTATIONAL PROTOCOL

All DFT calculations in this study have been performed using the Gaussian 16 suite of ab initio programs[42] employing the hybrid XC functional B3PW91.[43] This functional has been proven to give more reliable intermolecular interaction energy than other functionals,[44] such as the most popular B3LYP[38a)] functional, for complexes involving strongly bound ionic hydrogen bonds such as those involved in our systems.

Preliminary calculations were performed anyway by employing the hybrid B3LYP[39a)] functional and ω-B97XD functional,[38b)] which uses a version of Grimme's D2 dispersion mode developed to properly take weak interactions into consideration, to test the reliability of the B3PW91 results for the specific system under investigation. The energy barriers for the epoxide opening step through the α and β routes have been calculated using all the three abovementioned functionals. The results, shown in Table S1 in the Supporting Information, confirmed the α route as the favored one. Particularly, the B3PW91 and B3LYP functionals give very similar energy barriers, confirming that replacing the VWN and LYP correlation functional in B3LYP with the Perdew/Wang 91 correlation functionals in B3PW91 has no effect for this specific system, while the inclusion of dispersion corrections in ω-B97XD functional seems to overestimate the energy barriers.

Frequency calculations at the same level of theory were also performed to identify all stationary points as minima (zero imaginary frequencies) or transition states (one imaginary frequency).

Standard 6-31+G** basis sets of Pople and coworkers were used for all atoms except iodine, I, for which the relativistic compact Stuttgart/Dresden effective core potential[45] has been used in conjunction with its split valence basis set.

For transition states we carefully checked that the vibrational mode associated with the imaginary frequency corresponded to the correct movement of the involved atoms. Furthermore, the intrinsic reaction coordinate (IRC)[46] method was used to check that the localized TSs correctly connect to the corresponding minima along the imaginary mode of vibration.

While the results in this work do not account for solvent effects, the validity of this protocol was verified by additional simulations (for more details, see S7 section in the Supporting Information). Both, a CPCM and explicit solvent model were applied for comparison. The commonly used CPCM[47] approach was found to be not reliable, which can be expected as the solvent is actively participating in the reaction mechanism. Nevertheless, these preliminary studies have also shown that here is good agreement between the gas-phase free energy barriers reported in the paper and those calculated using the explicit solvent model, underlying the reliability of the presented results and offering further information that can be directly compared with other studies where solvent effects were not considered.[11,22d),e),27c)] A systematic discussion of potential solvent effects using an explicit approach is beyond the scope here and will be left for future works.

■ ASSOCIATED CONTENT

Supporting Information

The Supporting Information is available free of charge at https://pubs.acs.org/doi/10.1021/acsomega.0c01572.

Atomic coordinates and free energies of all optimized stationary points and transition states (PDF)

■ AUTHOR INFORMATION

Corresponding Author

Valeria Butera − *Central European Institute of Technology, CEITEC, Brno 612 00, Czech Republic;* orcid.org/0000-0002-4344-8118; Email: valeria.butera@ceitec.vutbr.cz

Author

Hermann Detz − *Central European Institute of Technology, CEITEC, Brno 612 00, Czech Republic; Center for Micro- and Nanostructures & Institute of Solid State Electronics, TU Wien, 1040 Vienna, Austria*

Complete contact information is available at: https://pubs.acs.org/10.1021/acsomega.0c01572

Author Contributions

V.B. performed the DFT simulations and analysis. Both authors contributed to the manuscript.

Funding

This research was carried out under the project CEITEC 2020 (LQ1601) with financial support from the Ministry of Education, Youth and Sports of the Czech Republic under the National Sustainability Programme II.

Notes

The authors declare no competing financial interest.

■ REFERENCES

(1) Aresta, M. *Carbon Dioxide as Chemical Feedstock*; Wiley-VCH: Weinheim, 2010.

(2) Peters, M.; Kçhler, B.; Kuckshinrichs, W.; Leitner, W.; Markewitz, P.; Müller, T. E. Cover Picture: Chemical Technologies for Exploiting and Recycling Carbon Dioxide into the Value Chain. *ChemSusChem* **2011**, *4*, 1216.

(3) Sakakura, T.; Kohno, K. The synthesis of organic carbonates from carbon dioxide. *Chem. Commun.* **2009**, 1312.

(4) Sakakura, T.; Choi, J.-C.; Yasuda, H. Transformation of Carbon Dioxide. *Chem. Rev.* **2007**, *107*, 2365.

(5) Cokoja, M.; Bruckmeier, C.; Rieger, B.; Herrmann, W. A.; Kühn, F. E. Transformation of carbon dioxide with homogeneous transition-metal catalysts: a molecular solution to a global challenge? *Angew. Chem. Int. Ed.* **2011**, *50*, 8510.

(6) Centi, G.; Iaquaniello, G.; Perathoner, S. Can We Afford to Waste Carbon Dioxide? Carbon Dioxide as a Valuable Source of Carbon for the Production of Light Olefins. *ChemSusChem* **2011**, *4*, 1265.

(7) Sheldon, R. A.; Arends, I.; Hanefeld, U. *Green Chemistry and Catalysis*; Wiley-VCH: Weinheim, 2007.

(8) Decortes, A.; Castilla, A. M.; Kleij, A. W. Salen-complex-mediated formation of cyclic carbonates by cycloaddition of CO_2 to epoxides. *Angew. Chem., Int. Ed.* **2010**, *49*, 9822.

(9) Sun, J.; Wang, J. Q.; Cheng, W. G.; Zhang, J. X.; Li, X. H.; Zhang, S. J.; She, Y. B. Chitosan functionalized ionic liquid as a recyclable biopolymer-supported catalyst for cycloaddition of CO_2. *Green Chem.* **2012**, *14*, 654.

(10) Yang, Z.-Z.; He, L.-N.; Miao, C.-X.; Chanfreaua, S. Lewis Basic Ionic Liquids-Catalyzed Conversion of Carbon Dioxide to Cyclic Carbonates. *Adv. Synth. Catal.* **2010**, *352*, 2233.
(11) Wang, J.-Q.; Dong, K.; Cheng, W.-G.; Sun, J.; Zhang, S. J. Insights into quaternary ammonium salts-catalyzed fixation carbon dioxide with epoxides. *Catal. Sci. Technol.* **2012**, *2*, 1480.
(12) Ren, Y.; Guo, C. H.; Jia, J. F.; Wu, H. S. A Computational Study on the Chemical Fixation of Carbon Dioxide with Epoxide Catalyzed by LiBr Salt. *J. Phys. Chem. A.* **2011**, *115*, 2258.
(13) Foltran, S.; Méreau, R.; Tassaing, T. On the interaction between supercritical CO2 and epoxides combining infrared absorption spectroscopy and quantum chemistry calculations. *Phys. Chem. Chem. Phys.* **2011**, *13*, 9209.
(14) Guo, C.-H.; Wu, H.-S.; Zhang, X.-M.; Song, J.-Y.; Zhang, X. A Comprehensive Theoretical Study on the Coupling Reaction Mechanism of Propylene Oxide with Carbon Dioxide Catalyzed by Copper(I) Cyanomethyl. *J. Phys. Chem. A.* **2009**, *113*, 6710.
(15) Man, M. L.; Lam, K. C.; Sit, W. N.; Ng, S. M.; Zhou, Z.; Lin, Z.; Lau, C. P. Synthesis of Heterobimetallic Ru-Mn Complexes and the Coupling Reactions of Epoxides with Carbon Dioxide Catalyzed by these Complexes. *Chem. − Eur. J.* **2006**, *12*, 1004.
(16) Guo, C.-H.; Zhang, X.-M.; Jia, J.-F.; Wu, H.-S. Theoretical study on the mechanism of nickel(0)-mediated coupling between carbon dioxide and epoxyethane. *THEOCHEM* **2009**, *916*, 125.
(17) Schäffner, B.; Schäffner, F.; Verevkin, S. P.; Börner, A. Organic carbonates as solvents in synthesis and catalysis. *Chem. Rev.* **2010**, *110*, 4554.
(18) North, M.; Pizzato, F.; Villuendas, P. Organocatalytic, asymmetric aldol reactions with a sustainable catalyst in a green solvent. *ChemSusChem* **2009**, *2*, 862.
(19) Scrosati, B.; Hassoun, J.; Sun, Y.-K. Lithium-ion batteries A look into the future. *Energy Environ. Sci.* **2011**, *4*, 3287.
(20) Li, Y.; Junge, K.; Beller, M. Improving the Efficiency of the Hydrogenation of Carbonates and Carbon Dioxide to Methanol. *ChemCatChem* **2013**, *5*, 1072.
(21) Yadollahi, M.; Bouhendi, H.; Zohuriaan-Mehr, M. J.; Farhadnejad, H.; Kabiri, K. Investigation of viscoelastic and thermal properties of cyclic carbonate bearing copolymers. *Polym. Sci. B.* **2013**, *55*, 327.
(22) (a)) Sun, J.; Fujita, S.-i.; Arai, M. J. Development in the green synthesis of cyclic carbonate from carbon dioxide using ionic liquids. *Organomet. Chem.* **2005**, *690*, 3490. (b)) Zhao, Y.; Yao, C.; Chen, G.; Yuan, Q. Highly efficient synthesis of cyclic carbonate with CO_2 catalyzed by ionic liquid in a microreactor. *Green Chem.* **2013**, *15*, 446. (c)) Girard, A.-L.; Simon, N.; Zanatta, M.; Marmitt, S.; Gonçalves, P.; Dupont, J. Insights on recyclable catalytic system composed of task-specific ionic liquids for the chemical fixation of carbon dioxide. *Green Chem.* **2014**, *16*, 2815. (d)) Sun, H.; Zhang, D. Density Functional Theory Study on the Cycloaddition of Carbon Dioxide with Propylene Oxide Catalyzed by Alkylmethylimidazolium Chlorine Ionic Liquids. *J. Phys. Chem. A* **2007**, *111*, 8036−8043. (e)) Marmitt, S.; Gonçalves, P. F. B. A DFT study on the insertion of CO_2 into styrene oxide catalyzed by 1-butyl-3-methyl-Imidazolium bromide ionic liquid. *J. Comput. Chem.* **2015**, *36*, 1322−1333.
(23) (a)) Paddock, R. L.; Nguyen, S. T. Chiral (salen)Co^{III}catalyst for the synthesis of cyclic carbonates. *Chem. Commun.* **2004**, 1622. (b)) Whiteoak, C. J.; Martin, E.; Martinez Belmonte, M.; Benet-Buchholz, J.; Kleij, A. W. An efficient iron catalyst for the synthesis of five- and six-membered organic carbonates under mild conditions. *Adv. Synth. Catal.* **2012**, *354*, 469. (c)) Haak, R. M.; Decortes, A.; Escudero-Adán, E. C.; Martinez Belmonte, M.; Martin, E.; Benet-Buchholz, J.; Kleij, A. W. Shape-Persistent Octanuclear Zinc Salen Clusters: Synthesis, Characterization, and Catalysis. *Inorg. Chem.* **2011**, *50*, 7934. (d)) North, M.; Pasquale, R. Mechanism of cyclic carbonate synthesis from epoxides and CO_2. *Angew. Chem. Int. Ed.* **2009**, *48*, 2946. (e)) Decortes, A.; Martinez Belmonte, M.; Benet-Buchholz, J.; Kleij, A. W. Efficient carbonate synthesis under mild conditions through cycloaddition of carbon dioxide to oxiranes using a Zn(salphen) catalyst. *Chem. Commun.* **2010**, *46*, 4580. (f)) Langanke, J.; Greiner, L.; Leitner, W. Substrate dependent synergetic and antagonistic interaction of ammonium halide and polyoxometalate catalysts in the synthesis of cyclic carbonates from oleochemical epoxides and CO_2. *Green Chem.* **2013**, *15*, 1173. (g)) Whiteoak, C. J.; Kielland, N.; Laserna, V.; Castro-Gomez, F.; Martin, E.; Escudero-Adann, E. C. C.; Kleij, A. W. Highly Active Aluminium Catalysts for the Formation of Organic Carbonates from CO2 and Oxiranes. *Chem. − Eur. J.* **2014**, *20*, 2264.
(24) (a)) Buchard, A.; Kember, M. R.; Sandeman, K. G.; Williams, C. K. A bimetallic iron(III) catalyst for CO_2/epoxide coupling. *Chem. Commun.* **2011**, *47*, 212. (b)) Ema, T.; Miyazaki, Y.; Koyama, S.; Yano, Y.; Sakai, T. A bifunctional catalyst for carbon dioxide fixation: cooperative double activation of epoxides for the synthesis of cyclic carbonates. *Chem. Commun.* **2012**, *48*, 4489. (c)) Escárcega-Bobadilla, M. V.; Martinez Belmonte, M.; Martin, E.; Escudero-Adán, E. C.; Kleij, A. W. A Recyclable Trinuclear Bifunctional Catalyst Derived from a Tetraoxo BisZn(salphen) Metalloligand. *Chem. − Eur. J.* **2013**, *19*, 2641. (d)) Meléndez, J.; North, M.; Villuendas, P.; Young, C. One-component bimetallic aluminium(salen)-based catalysts for cyclic carbonate synthesis and their immobilization. *Dalton. Trans.* **2011**, *40*, 3885. (e)) Fuchs, M. A.; Zevaco, T. A.; Ember, E.; Walter, O.; Held, I.; Dinjus, E.; Döring, M. Synthesis of cyclic carbonates from epoxides and carbon dioxide catalyzed by an easy-to-handle ionic iron(III) complex. *Dalton Trans.* **2013**, *42*, 5322.
(25) (a)) Caló, V.; Nacci, A.; Monopoli, A.; Fanizzi, A. Cyclic Carbonate Formation from Carbon Dioxide and Oxiranes in Tetrabutylammonium Halides as Solvents and Catalysts. *Org. Lett.* **2002**, *4*, 2561. (b)) Montoyaa, C. A.; Paninhoa, A. B.; Felixa, P. M.; Zakrzewskaa, M. E.; Vitala, J.; Najdanovic-Visakb, V.; Nunes, A. V. M. Styrene carbonate synthesis from CO_2 using tetrabutylammonium bromide as a non-supported heterogeneous catalyst phase. *J. Supercrit. Fluids* **2015**, *100*, 155.
(26) Butera, V.; Russo, N.; Cosentino, U.; Greco, C.; Moro, G.; Pitea, D.; Sicilia, E. Computational Insight on CO_2 Fixation to Produce Styrene Carbonate Assisted by a Single-Center Aluminum-(III) Catalyst and Quaternary Ammonium Salts. *ChemCatChem* **2016**, *8*, 1167.
(27) (a)) Whiteoak, C. J.; Nova, A.; Maseras, F.; Kleij, A. W. Merging sustainability with organocatalysis in the formation of organic carbonates by using CO_2 as a feedstock. *ChemSusChem* **2012**, *5*, 2032. (b)) Wang, J.-Q.; Sun, J.; Cheng, W.-C.; Dong, K.; Zhang, X.-P.; Zhang, S.-J. Experimental and theoretical studies on hydrogen bond-promoted fixation of carbon dioxide and epoxides in cyclic carbonates. *Phys. Chem. Chem. Phys.* **2012**, *14*, 11021−11026. (c)) Alves, M.; Mereau, R.; Grignard, B.; Detrembleur, C.; Jerome, C.; Tassaing, T. A comprehensive density functional theory study of the key role of fluorination and dual hydrogen bonding in the activation of the epoxide/CO_2 coupling by fluorinated alcohols. *RSC Adv.* **2016**, *6*, 36327−36335.
(28) (a) Ma, J.; Liu, J.; Zhang, Z.; Han, B. The catalytic mechanism of KI and the co-catalytic mechanism of hydroxyl substances for cycloaddition of CO_2 with propylene oxide. *GreenChem.* **2012**, *14*, 2410.
(29) Lee, J. W.; Yan, H.; Jang, H. B.; Kim, H. K.; Park, S.-W.; Lee, S.; Chi, D. Y.; Song, C. E. Bis-terminal hydroxy polyethers as all-purpose, multifunctional organic promoters: a mechanistic investigation and applications. *Angew. Chem. Int. Ed.* **2009**, *48*, 7683.
(30) Kaneko, S.; Shirakawa, S. Potassium Iodide−Tetraethylene Glycol Complex as a Practical Catalyst for CO_2 Fixation Reactions with Epoxides under Mild Conditions. *ACS Sustainable Chem. Eng.* **2017**, *5*, 2836.
(31) Yanagida, S.; Takahashi, K.; Okahara, M. Metal-ion Complexation of Noncyclic Poly(oxyethylene) Derivatives Complexation in Aprotic Solvent and Isolation of Their Solid Complexes. *Bull. Chem. Soc. Jpn.* **1978**, *51*, 1294.
(32) Vögtle, F.; Weber, E. Multidentate Acyclic Neutral Ligands and Their Complexation. *Angew. Chem., Int. Ed. Engl.* **1979**, *18*, 753.
(33) Okada, T. Complexation of poly(oxyethylene) in analytical chemistry. A review. *Analyst* **1993**, *118*, 959.

https://dx.doi.org/10.1021/acsomega.0c01572
ACS Omega 2020, 5, 18064−18072

(34) Sawada, K.; Imai, A.; Satoh, K.; Kikuchi, Y. Structures of Linear Poly(ethylene oxide) Compounds and Potassium Complexes in Dichloromethane. *J. Phys. Chem. B.* **2007**, *111*, 4361.
(35) Jadhav, V. H.; Kim, J. G.; Park, S. H.; Kim, D. W. Task-specific hexaethylene glycol bridged di-cationic ionic liquids as catalysts for nucleophilic fluorination using potassium fluoride. *Chem. Eng. J.* **2017**, *308*, 664.
(36) Jadhav, V. H.; Jang, S. H.; Jeong, H.-J.; Lim, S. T.; Sohn, M.-H.; Kim, J.-Y.; Lee, S.; Lee, J. W.; Song, C. E.; Kim, D. W. Oligoethylene Glycols as Highly Efficient Mutifunctional Promoters for Nucleophilic-Substitution Reactions. *Chem. − Eur. J.* **2012**, *18*, 3918.
(37) Hasaninejad, A.; Beyrati, M. Eco-friendly polyethylene glycol (PEG-400): a green reaction medium for one-pot, four-component synthesis of novel asymmetrical bis-spirooxindole derivatives at room temperature. *RSC Adv.* **2018**, *8*, 1934.
(38) (a)) Becke, A. D. Density-functional thermochemistry. III. The role of exact exchange. *J. Chem. Phys.* **1993**, *98*, 5648−5652. (b)) Stephens, P. J.; Devlin, F. J.; Chabalowski, C. F.; Frisch, M. J. Ab Initio Calculation of Vibrational Absorption and Circular Dichroism Spectra Using Density Functional Force Fields. *J. Phys. Chem.* **1994**, *98*, 11623−11627. (c)) Becke, A. D. Density-functional thermochemistry. V. Systematic optimization of exchange-correlation functionals. *J. Chem. Phys.* **1997**, *107*, 8554.
(39) (a)) Foster, J. P.; Weinhold, F. Natural hybrid orbitals. *J. Am. Chem. Soc.* **1980**, *102*, 7211. (b)) Reed, A. E.; Weinstock, R. B.; Weinhold, F. Natural population analysis. *J. Chem. Phys.* **1985**, *83*, 735. (c)) Reed, A. E.; Weinhold, F. Natural localized molecular orbitals. *J. Chem. Phys.* **1985**, *83*, 1736. (d)) Carpenter, J. E.; Weinhold, F. Analysis of the geometry of the hydroxymethyl radical by the "different hybrids for different spins" natural bond orbital procedure. *J. Mol. Struct.* **1988**, *169*, 41. (e)) Reed, A. E.; Curtiss, L. A.; Weinhold, F. Intermolecular interactions from a natural bond orbital, donor-acceptor viewpoint. *Chem. Rev.* **1988**, *88*, 899.
(40) (a)) Hirshfeld, F. L. Bonded-atom fragments for describing molecular charge densities. *Theor. Chem. Acc.* **1977**, *44*, 129. (b)) Ritchie, J. P. Electron density distribution analysis for nitromethane, nitromethide, and nitramide. *J. Am. Chem. Soc.* **1985**, *107*, 1829. (c)) Ritchie, J. P.; Bachrach, S. M. Some methods and applications of electron density distribution analysis. *J. Comput. Chem.* **1987**, *8*, 499.
(41) Comerford, J. W.; Ingram, I. D. V.; North, M.; Wu, X. Sustainable metal-based catalysts for the synthesis of cyclic carbonates containing five-membered rings. *Green Chem.* **2015**, *17*, 1966.
(42) Frisch, M. J.; Trucks, G. W.; Schlegel, H. B.; Scuseria, G. E.; Robb, M. A.; Cheeseman, J. R.; Scalmani, G.; Barone, V.; Petersson, G. A.; Nakatsuji, H.; Li, X.; Caricato, M.; Marenich, A. V.; Bloino, J.; Janesko, B. G.; Gomperts, R.; Mennucci, B.; Hratchian, H. P.; Ortiz, J. V.; Izmaylov, A. F.; Sonnenberg, J. L.; Williams-Young, D.; Ding, F.; Lipparini, F.; Egidi, F.; Goings, J.; Peng, B.; Petrone, A.; Henderson, T.; Ranasinghe, D.; Zakrzewski, V. G.; Gao, J.; Rega, N.; Zheng, G.; Liang, W.; Hada, M.; Ehara, M.; Toyota, K.; Fukuda, R.; Hasegawa, J.; Ishida, M.; Nakajima, T.; Honda, Y.; Kitao, O.; Nakai, H.; Vreven, T.; Throssell, K.; Montgomery, J. A., Jr.; Peralta, J. E.; Ogliaro, F.; Bearpark, M. J.; Heyd, J. J.; Brothers, E. N.; Kudin, K. N.; Staroverov, V. N.; Keith, T. A.; Kobayashi, R.; Normand, J.; Raghavachari, K.; Rendell, A. P.; Burant, J. C.; Iyengar, S. S.; Tomasi, J.; Cossi, M.; Millam, J. M.; Klene, M.; Adamo, C.; Cammi, R.; Ochterski, J. W.; Martin, R. L.; Morokuma, K.; Farkas, O.; Foresman, J. B.; Fox, D. J. *Gaussian 16*, Revision C.01, Gaussian, Inc.: Wallingford CT, 2016.
(43) (a)) Becke, A. D. Density-functional thermochemistry. III. The role of exact exchange. *J. Chem. Phys.* **1993**, *98*, 5648. (b)) Perdew, J. P.; Wang, Y. Accurate and simple analytic representation of the electron-gas correlation energy. *Phys. Rev. B* **1992**, *45*, 13244.
(44) Milet, A.; Korona, T.; Moszynski, R.; Kochanski, E. Anisotropic intermolecular interactions in van der Waals and hydrogen-bonded complexes: What can we get from density functional calculations? *J. Chem. Phys.* **1999**, *111*, 7727.
(45) Andrae, D.; Häußermann, U.; Dolg, M.; Stoll, H.; Preuß, H. Energy-adjustedab initio pseudopotentials for the second and third row transition elements. *Theor. Chim. Acta* **1990**, *77*, 123.
(46) (a)) Fukui, K. Formulation of the reaction coordinate. *J. Phys. Chem.* **1970**, *74*, 4161. (b)) Gonzalez, C.; Schlegel, H. B. An improved algorithm for reaction path following. *J. Chem. Phys.* **1989**, *90*, 2154.
(47) Barone, V.; Cossi, M. Quantum Calculation of Molecular Energies and Energy Gradients in Solution by a Conductor Solvent Model. *J. Phys. Chem. A.* **1998**, *102*, 1995−2001.

https://dx.doi.org/10.1021/acsomega.0c01572
ACS Omega 2020, 5, 18064−18072